

MICROBUNCHING INSTABILITY MITIGATION VIA MULTI-STAGE CANCELLATION

Biaobin Li^{1,2}, Ji Qiang^{2,*}

¹ University of Science and Technology of China, [230029] Hefei, China

² Lawrence Berkeley National Laboratory, [94720] Berkeley, USA

ABSTRACT

The microbunching instability driven by beam collective effects in the linear accelerator of a free electron laser (FEL) facility can significantly degrade electron beam quality and FEL performance. Understanding and control of the instability is a priority for the design of modern high-brightness electron accelerators. In this paper, we study an instability cancellation phenomenon due to 180° phase slippage of the current modulations between different amplification stages. A case study of using a nonisochronous dogleg section in a double compression scheme to cancel the current modulation is illustrated.

INTRODUCTION

The microbunching instability (MBI) in linacs can limit the performance of high-brightness linac-driven light sources such as free electron lasers by degrading the beam quality. The instability stems from some small undesired density fluctuations, and then get amplified by the energy modulations induced by the collective effects when the beam transfers through dispersive regions with nonzero R_{56} [1–3]. A number of methods have been proposed to mitigate the instability by using a laser heater to increase the beam uncorrelated energy spread before bunch compressors [4, 5] or by using transverse-to-longitudinal coupling from dispersive elements [6–10].

For multi-stage amplifications that consists of two bunch compressors (BCs) and a nonisochronous dogleg, we observed a microbunching gain cancellation phenomenon due to the phase slippages of the current and energy modulations between different amplification stages. And this may result in instability cancellation rather than the high-gain klystron-like amplification process [1]. In this paper, we consider an FEL linac with double compression scheme and derive the analytical expressions of the multi-stage amplification or cancellation mechanisms. As an illustration, we use a dogleg section with nonzero R_{56} to mitigate the instability.

PRINCIPLES OF MULTI-STAGE CANCELLATION

To understand the cancellation mechanism, let's first consider a simple model with lattice arrangements of (drift 1, BC1, drift 2, BC2), where no bunch length compression is involved. The evolution of current and energy modulation is plotted in Fig. 1. The electron beam with initial current modulation induces energy modulation due to LSC effects

after traveling through drift 1. And then, energy modulation is transformed into density modulation after the electron beam passes through BC1, where we can see 180° phase slippages of the density profile compared with the initial current modulation. Repeating this process, by proper choosing the value of momentum compaction factor R_{56} in BC2, we can smooth the final density profile by making use of the 180° phase slippages after BC2, due to the fact that LSC impedance is purely imaginary. This simple model indicates that by careful design of the facility, microbunching instability may be mitigated after multi-stage transportation.

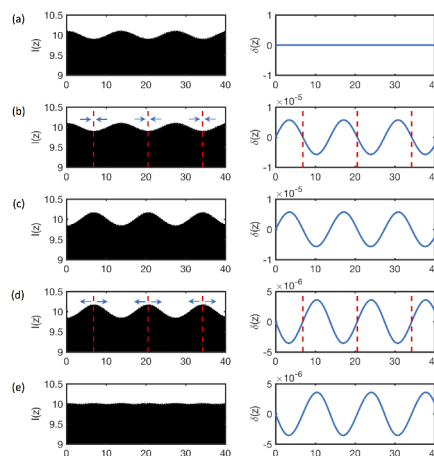


Figure 1: (color online). Illustration of current (left column) and energy (right column) modulation evolution. (a)–(e), modulations of the initial, after drift 1, after BC1, after drift 2, after BC2 respectively. The bunch length is in unit of mm, and current in unit of A.

Now let's consider a more practical case shown in Fig. 2, consisting of two bunch compressors BC1 and BC2 followed by a dogleg inserted with several quadrupoles, which ensures a tunable strength of momentum compaction factor $R_{56,3}$. In the following we consider only LSC effects which dominate the microbunching instability amplification [4], and assumed frozen beam model with electron longitudinal locations unchanged during the transportation in linacs [11]. The density modulation is governed by the Volterra integral equation described in [2, 3]. By iterating the microbunching integral equation thrice, we can obtain the final modulation

* jqiang@lbl.gov

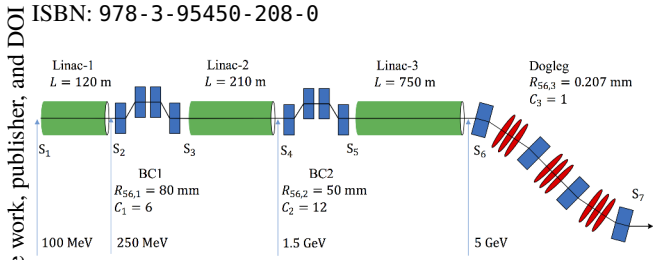


Figure 2: (color online). Scheme Layout.

factor as

$$\begin{aligned}
 b[k(s); s] &= b^{(0)}[k(s); s] + \int_0^s d\tau K(\tau, s) b^{(0)}[K(\tau); \tau] \\
 &+ \int_0^s d\tau K(\tau, s) \int_0^\tau d\zeta K(\zeta, \tau) b^{(0)}[K(\zeta); \zeta] \\
 &+ \int_0^s d\tau K(\tau, s) \int_0^\tau d\zeta K(\zeta, \tau) \\
 &\times \int_0^\zeta dt K(t, \zeta) b^{(0)}[K(t); t],
 \end{aligned} \quad (1)$$

where $K(\tau, s)$ is the integral kernel defined in [12] in the presence of acceleration, $b^{(0)}[k(s); s]$ is the bunching factor degradation solely from the transportation of beam optics. Assuming an electron beam with an initial current modulation factor b_0 at the entrance s_1 to Linac-1, the final modulation factor after dogleg by applying Eq. 1 can be given as

$$\begin{aligned}
 b[k(s_7); s_7] &= b_{01}[k(s_7); s_7] + b_{11}[k(s_7); s_7] + b_{12}[k(s_7); s_7] \\
 &+ b_{13}[k(s_7); s_7] + b_{21}[k(s_7); s_7] + b_{22}[k(s_7); s_7] \\
 &+ b_{23}[k(s_7); s_7] + b_{31}[k(s_7); s_7],
 \end{aligned} \quad (2)$$

where $k(s) = C(s)k_0$, $C(s)$ is the compression factor, k_0 is the initial modulation wave number. Here b_{01} describes the evolution of the modulation factor in the absence of all collective effects, and is given as

$$b_{01}[k(s_7); s_7] = b_0 \exp[-k^2(s_7) \hat{R}_{56}^2(s_{1 \rightarrow 7}) \sigma_{\delta_0}^2 / 2]; \quad (3)$$

the three terms of b_{11} , b_{12} , b_{13} describe the one-stage amplification of the initial microbunching due to the collective effects between the linac sections of $s_{1 \rightarrow 2}$, $s_{3 \rightarrow 4}$, $s_{5 \rightarrow 6}$ respectively, and are given as

$$\begin{aligned}
 b_{11}[k(s_7); s_7] &= ib_0 k(s_7) \hat{R}_{56}(s_{1 \rightarrow 7}) \frac{I(s_1)}{\gamma_0} \hat{Z}(s_{1 \rightarrow 2}) \\
 &\times \exp\left(\frac{-k_0^2 \mathcal{D}^2(s_{1 \rightarrow 7}) \sigma_{\delta_0}^2}{2}\right),
 \end{aligned} \quad (4)$$

$$\begin{aligned}
 b_{12}[k(s_7); s_7] &= ib_0 k(s_7) \hat{R}_{56}(s_{3 \rightarrow 7}) \frac{I(s_3)}{\gamma_0} \hat{Z}(s_{3 \rightarrow 4}) \\
 &\times \exp\left(\frac{-k_0^2 \mathcal{D}^2(s_{3 \rightarrow 7}) \sigma_{\delta_0}^2}{2}\right),
 \end{aligned} \quad (5)$$

$$\begin{aligned}
 b_{13}[k(s_7); s_7] &= ib_0 k(s_7) \hat{R}_{56}(s_{5 \rightarrow 7}) \frac{I(s_5)}{\gamma_0} \hat{Z}(s_{5 \rightarrow 6}) \\
 &\times \exp\left(\frac{-k_0^2 \mathcal{D}^2(s_{5 \rightarrow 7}) \sigma_{\delta_0}^2}{2}\right);
 \end{aligned} \quad (6)$$

the following three terms b_{21} , b_{22} , b_{23} describe the two-stage amplifications due to coupled collective effects between the region $s_{1 \rightarrow 2}$ and $s_{3 \rightarrow 4}$, $s_{1 \rightarrow 2}$ and $s_{5 \rightarrow 6}$, $s_{3 \rightarrow 4}$ and $s_{5 \rightarrow 6}$ respectively, and are given as

$$\begin{aligned}
 b_{21}[k(s_7); s_7] &= -b_0 k(s_3) k(s_7) \hat{R}_{56}(s_{1 \rightarrow 3}) \hat{R}_{56}(s_{3 \rightarrow 7}) \\
 &\times \frac{I(s_1) I(s_3)}{(\gamma_0)^2} \hat{Z}(s_{1 \rightarrow 2}) \hat{Z}(s_{3 \rightarrow 4}) \\
 &\times \exp\left(\frac{-k_0^2 \mathcal{D}^2(s_{1 \rightarrow 3 \rightarrow 7}) \sigma_{\delta_0}^2}{2}\right),
 \end{aligned} \quad (7)$$

$$\begin{aligned}
 b_{22}[k(s_7); s_7] &= -b_0 k(s_5) k(s_7) \hat{R}_{56}(s_{1 \rightarrow 5}) \hat{R}_{56}(s_{5 \rightarrow 7}) \\
 &\times \frac{I(s_1) I(s_5)}{(\gamma_0)^2} \hat{Z}(s_{1 \rightarrow 2}) \hat{Z}(s_{5 \rightarrow 6}) \\
 &\times \exp\left(\frac{-k_0^2 \mathcal{D}^2(s_{1 \rightarrow 5 \rightarrow 7}) \sigma_{\delta_0}^2}{2}\right),
 \end{aligned} \quad (8)$$

$$\begin{aligned}
 b_{23}[k(s_7); s_7] &= -b_0 k(s_5) k(s_7) \hat{R}_{56}(s_{3 \rightarrow 5}) \hat{R}_{56}(s_{5 \rightarrow 7}) \\
 &\times \frac{I(s_3) I(s_5)}{(\gamma_0)^2} \hat{Z}(s_{3 \rightarrow 4}) \hat{Z}(s_{5 \rightarrow 6}) \\
 &\times \exp\left(\frac{-k_0^2 \mathcal{D}^2(s_{3 \rightarrow 5 \rightarrow 7}) \sigma_{\delta_0}^2}{2}\right);
 \end{aligned} \quad (9)$$

the last term denotes the three-stage cascade amplification due to the collective effects between the region $s_{1 \rightarrow 2}$ and $s_{3 \rightarrow 4}$ and $s_{5 \rightarrow 6}$, and is given as

$$\begin{aligned}
 b_{31}[k(s_7); s_7] &= -ib_0 k(s_3) k(s_5) k(s_7) \hat{R}_{56}(s_{1 \rightarrow 3}) \\
 &\times \hat{R}_{56}(s_{3 \rightarrow 5}) \hat{R}_{56}(s_{5 \rightarrow 7}) \frac{I(s_1) I(s_3) I(s_5)}{(\gamma_0)^3} \\
 &\times \hat{Z}(s_{1 \rightarrow 2}) \hat{Z}(s_{3 \rightarrow 4}) \hat{Z}(s_{5 \rightarrow 6}) \\
 &\times \exp\left(\frac{-k_0^2 \mathcal{D}^2(s_{1 \rightarrow 3 \rightarrow 5 \rightarrow 7}) \sigma_{\delta_0}^2}{2}\right).
 \end{aligned} \quad (10)$$

The impedance term above is defined as

$$\hat{Z}(s_{j \rightarrow k}) = \int_{s_j}^{s_k} \frac{4\pi Z[k(\tau); \tau]}{I_A Z_0} d\tau,$$

where $Z[k(\tau); \tau]$ is the impedance per unit length of collective effects and Z_0 is the vacuum impedance, I_A is the Alfvén current, σ_{δ_0} is the initial rms relative energy spread, γ_0 is the initial electron beam relativistic factor, $I(s_j) = C(s_j)I_0$, I_0 is the initial current. The exponential damping to the modulation amplification due to initial energy spread is given by

$$\begin{aligned}
 \mathcal{D}^2(s_{1 \rightarrow 7}) &= U^2(s_7, s_1), \\
 \mathcal{D}^2(s_{3 \rightarrow 7}) &= U^2(s_7, s_3) + U^2(s_3, s_1), \\
 \mathcal{D}^2(s_{5 \rightarrow 7}) &= U^2(s_7, s_5) + U^2(s_5, s_1), \\
 \mathcal{D}^2(s_{1 \rightarrow 3 \rightarrow 7}) &= U^2(s_7, s_3) + U^2(s_3, s_1), \\
 \mathcal{D}^2(s_{1 \rightarrow 5 \rightarrow 7}) &= U^2(s_7, s_5) + U^2(s_5, s_1), \\
 \mathcal{D}^2(s_{3 \rightarrow 5 \rightarrow 7}) &= U^2(s_7, s_5) + U^2(s_5, s_3) + U^2(s_3, s_1), \\
 \mathcal{D}^2(s_{1 \rightarrow 3 \rightarrow 5 \rightarrow 7}) &= U^2(s_7, s_5) + U^2(s_5, s_3) + U^2(s_3, s_1),
 \end{aligned} \quad (11)$$

where $U(s, \tau) = C(s)\hat{R}_{56}(s) - C(\tau)\hat{R}_{56}(\tau)$. We used the shorthand notation $\hat{R}_{56}(s) = \hat{R}_{56}(s_1 \rightarrow s)$ here. And $\hat{R}_{56}(s_j \rightarrow k)$ can be obtained by $\hat{R}_{56}(s_j \rightarrow k) = R_{56}(s_j \rightarrow k)\gamma_0/\gamma_j$, converted from the transfer matrix in (x, x', z, δ) coordinates in order to consider acceleration effects [12], and can be given as

$$\begin{aligned} \hat{R}_{56}(s_1) &= 0, \\ \hat{R}_{56}(s_1 \rightarrow 3) &= \frac{R_{56,1}\gamma_1}{\gamma_3}, \\ \hat{R}_{56}(s_1 \rightarrow 5) &= \frac{R_{56,1}\gamma_1}{C_2\gamma_3} + \frac{R_{56,2}C_1\gamma_1}{\gamma_5}, \\ \hat{R}_{56}(s_1 \rightarrow 7) &= \frac{R_{56,1}\gamma_1}{C_2C_3\gamma_3} + \frac{R_{56,2}C_1\gamma_1}{C_3\gamma_5} + \frac{R_{56,3}C_1C_2\gamma_1}{\gamma_7}, \quad (12) \\ \hat{R}_{56}(s_3 \rightarrow 5) &= \frac{R_{56,2}\gamma_1}{\gamma_5}, \\ \hat{R}_{56}(s_3 \rightarrow 7) &= \frac{R_{56,2}\gamma_1}{C_3\gamma_5} + \frac{R_{56,3}C_2\gamma_1}{\gamma_7}, \\ \hat{R}_{56}(s_5 \rightarrow 7) &= \frac{R_{56,3}\gamma_1}{\gamma_7}, \end{aligned}$$

where γ_j is the relativistic factor at location s_j .

A CASE STUDY

As the LSC impedance is purely imaginary, thus the one-stage amplification terms in Eq. 4-6 and three-stage amplification terms in Eq. 10 are all negative, the two-stage amplification terms in Eq. 7-9, however, are all positive, which indicate that the final gain may be cancelled by each other by proper lattice arrangements.

As an illustration of this method, we consider the detailed machine layout shown in Fig. 2. Energy chirp is created in Linac-1 and Linac-2, and then removed in Linac-3 which ensures no bunch length compression ($C_3 = 1$) in dogleg even if $R_{56,3}$ is non-zero. More detailed parameter settings are marked in Fig. 2. The initial electron beam transverse distribution is a uniform round cross section with 1 mm radius and with a flattop current of 15 A. For simple simulation benchmark with IMPACT [13], we assumed a zero transverse emittance to avoid using matching and FODO structures in linac sections to preserve the beam transverse size a constant value during the entire line. The initial uncorrelated energy spread is 2 keV with zero energy chirp. We modified the IMPACT source code to transport particles using first-order map to benchmark our analytical evaluations.

In order to use $R_{56,3}$ to mitigate the instability, we scanned $R_{56,3}$ to obtain the absolute gain $|b[k(s_7); s_7]/b_0|$ at different initial current modulation wavelengths shown in Fig. 3. The final density modulation originating from the initial $102\mu\text{m}$ density modulation wavelength is significantly suppressed when $R_{56,3} = 0.207\text{mm}$, which is illustrated in Fig. 4. The right plot in Fig. 4 shows the contributions of different amplification terms, which finally causes the cancellation of the total gain. Simulation results at short wavelength range show slight discrepancies between the analytical gain, which could

be due to the approximation involved in the space-charge impedance model used in the linear theory [14].

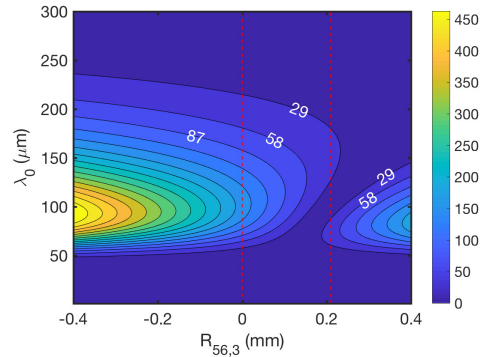


Figure 3: (color online). Microbunching gain (absolute value) as a function of the initial modulation wavelength λ_0 and $R_{56,3}$. Left and right dashed lines refer to $R_{56,3} = 0$ and $R_{56,3} = 0.207\text{mm}$ respectively.

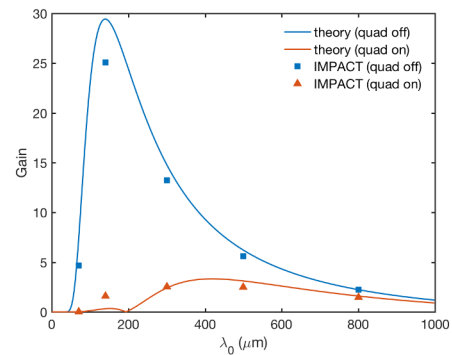


Figure 4: (color online). Left plot, microbunching gain (absolute value) as a function of the initial modulation wavelength λ_0 when $R_{56,3} = 0$ and $R_{56,3} = 0.207\text{mm}$. Right plot, contributions of each amplification term when $R_{56,3} = 0.207\text{mm}$, where $gain_{jk} = b_{jk}/b_0$.

CONCLUSIONS

Multi-stage MBI amplification analytical expressions are provided and benchmarked with IMPACT in this paper. Results show that by proper design of the FEL facility, the final microbunching gain could be mitigated due to the 180° phase slippages of the current modulations between different amplification stages.

ACKNOWLEDGMENTS

This work was supported by the U.S. Department of Energy under Contract No. DE-AC02-05CH11231. One of the authors, Biaobin Li, thanks China Scholarship Council for financial support (CSC File No. 201706340072).

REFERENCES

- [1] EL Saldin, EA Schneidmiller, and MV Yurkov. An analytical description of longitudinal phase space distortions in magnetic bunch compressors. *Nuclear Instruments and Methods in*

Physics Research Section A: Accelerators, Spectrometers, Detectors and Associated Equipment, 483(1-2):516–520, 2002.

- [2] Stupakov Heifets, G Stupakov, and S Krinsky. Coherent synchrotron radiation instability in a bunch compressor. *Physical Review Special Topics-Accelerators and Beams*, 5(6):064401, 2002.
- [3] Zhirong Huang and Kwang-Je Kim. Formulas for coherent synchrotron radiation microbunching in a bunch compressor chicane. *Physical Review Special Topics-Accelerators and Beams*, 5(7):074401, 2002.
- [4] EL Saldin, EA Schneidmiller, and MV Yurkov. Longitudinal space charge-driven microbunching instability in the tesla test facility linac. *Nuclear Instruments and Methods in Physics Research. Section A, Accelerators, Spectrometers, Detectors and Associated Equipment*, 528(1-2):355–359, 2004.
- [5] Zhirong Huang, A Brachmann, F-J Decker, Y Ding, D Dowell, P Emma, J Frisch, S Gilevich, G Hays, and Ph Hering. Measurements of the linac coherent light source laser heater and its impact on the x-ray free-electron laser performance. *Physical Review Special Topics-Accelerators and Beams*, 13(2):020703, 2010.
- [6] Christopher Behrens, Zhirong Huang, and Dao Xiang. Reversible electron beam heating for suppression of microbunching instabilities at free-electron lasers. *Physical Review Special Topics-Accelerators and Beams*, 15(2):022802, 2012.
- [7] Ji Qiang, Chad E Mitchell, and Marco Venturini. Suppression of microbunching instability using bending magnets in free-electron-laser linacs. *Physical review letters*, 111(5):054801, 2013.
- [8] Chao Feng, Dazhang Huang, Haixiao Deng, Qiang Gu, and Zhentang Zhao. Suppression of microbunching instability via a transverse gradient undulator. *New Journal of Physics*, 17(7):073028, 2015.
- [9] Dazhang Huang, Chao Feng, Haixiao Deng, Qiang Gu, and Zhentang Zhao. Transverse to longitudinal phase space coupling in an electron beam for suppression of microbunching instability. *Physical Review Accelerators and Beams*, 19(10):100701, 2016.
- [10] Tao Liu, Weilun Qin, Dong Wang, and Zhirong Huang. Reversible beam heater for suppression of microbunching instability by transverse gradient undulators. *Physical Review Accelerators and Beams*, 20(8):082801, 2017.
- [11] Zhirong Huang, M Borland, P Emma, J Wu, C Limborg, G Stupakov, and J Welch. Suppression of microbunching instability in the linac coherent light source. *Physical Review Special Topics-Accelerators and Beams*, 7(7):074401, 2004.
- [12] Marco Venturini. Microbunching instability in single-pass systems using a direct two-dimensional vlasov solver. *Physical Review Special Topics-Accelerators and Beams*, 10(10):104401, 2007.
- [13] Ji Qiang, Robert D Ryne, Salman Habib, and Viktor Decyk. An object-oriented parallel particle-in-cell code for beam dynamics simulation in linear accelerators. *Journal of Computational Physics*, 163(2):434–451, 2000.
- [14] J Qiang, RD Ryne, M Venturini, AA Zholents, and IV Pogorelov. High resolution simulation of beam dynamics in electron linacs for x-ray free electron lasers. *Physical Review Special Topics-Accelerators and Beams*, 12(10):100702, 2009.

Content from this work may be used under the terms of the CC BY 3.0 licence (© 2019). Any distribution of this work must maintain attribution to the author(s), title of the work, publisher, and DOI